

**Original scientific paper**

## COMPACT DUAL-BAND CIRCULARLY POLARIZED ANTENNA FOR WIRELESS COMMUNICATIONS

**Karunesh Srivastava<sup>1</sup>, Mayuri Kulshreshtha<sup>2</sup>**

<sup>1</sup>Department of Electronics & Communication Engineering  
Ajay Kumar Garg Engineering College Ghaziabad (U.P.), India

<sup>2</sup>Department of Computer Science & Engineering,  
IMS Engineering College Ghaziabad (U.P.), India

**Abstract.** *P-shaped dual-band circularly polarized (CP) antenna for wireless communications with right-hand circular polarization (RHCP) and left-hand circular polarization (LHCP) is presented in this article. Optimized electrical volume of the proposed structure is  $0.46\lambda_0 \times 0.46\lambda_0 \times 0.02\lambda_0$  mm<sup>3</sup> at 4.4 GHz resonant frequency. The measured -10 dB impedance bandwidths are 50.7% and 5.7% for (3.37-5.60 GHz) and (10.82-11.46 GHz) resonating bands at frequencies 4.4 GHz and 11.4 GHz respectively. The measured 3 dB impedance axial-ratio bandwidths for (4.65-5.13 GHz) and (11.21-11.52 GHz) bands are 9.7% and 2.7%. Agreement of simulation results with measured results ensure the excellent circular polarization at frequencies 4.96 GHz and 11.4 GHz.*

**Key words:** *Antenna, circularly polarized, C-Band, X-band, aeronautical mobile, satellite communication.*

### 1. INTRODUCTION

Multipath interferences and polarization losses are two main reasons for reduction of effect of linearly polarized (LP) antennas [1-3]. Circularly polarized (CP) antennas can receive all polarizations with outstanding feature of fairly constant signal strength, therefore circularly polarized antennas are used for reducing these losses. To design a circularly polarized antenna as compare to linearly polarized antenna is challenge in itself. In simulation environment, axial ratio is one of the important characteristics of circularly polarized antenna. Shape of the radiator, ground and feeding techniques play major role in achieving excellent axial ratio. Demand of compact dual/multiband CP antennas has increased manifolds. Numerous dual/multiband LP/CP antennas have been reported in [4-15] for different applications. Single and dual band circularly polarized antennas for various applications are reported. Tuned strip antenna with F-shaped ground [11], U-shaped patch antenna [12], CPW fed

---

Received March 23, 2023; revised May 01, 2023; accepted June 03, 2023

**Corresponding author:** Karunesh Srivastava

Ajay Kumar Garg Engineering College Ghaziabad (U.P.), India

E-mail: karunesh.ec@gmail.com

fork-shaped antenna [13], loaded square slot antenna with split ring resonators [14] have been reported to achieve dual-band circular polarization.

Numerous circularly polarized dual band antennas are encountered in reported literatures which are useful for different applications [16-17] as well as for C- and X-band applications [18-20]. A new design (evolution of [15]) of dual band circularly polarized antenna for C and X-band applications is proposed in this article.

Geometrical structure of the proposed design with physical dimensions is shown in Fig. 1. Frequency 4.4 GHz is chosen for calculating the electric size and for optimization of the proposed structure because maximum return loss (-35 dB) is observed in the simulation environment. P-shaped radiating patch with defected ground (incorporation of square track, square slot, slit and perturbation stub) is intuitively conceived from the literature and different techniques are used to obtain the optimized results. ANSYS HFSS version 13 is used for design and optimization purpose. Measurement is done for validating the simulation results. The proposed antenna is printed on the FR4-epoxy dielectric substrate having thickness  $h = 1.6$  mm, dielectric constant  $\epsilon = 4.4$  and loss of tangent  $\tan \delta = 0.02$ . Micro-strip feed line ( $\lambda_0/4$  mm) with  $50 \Omega$  characteristics impedance is used for excitation of proposed antenna.

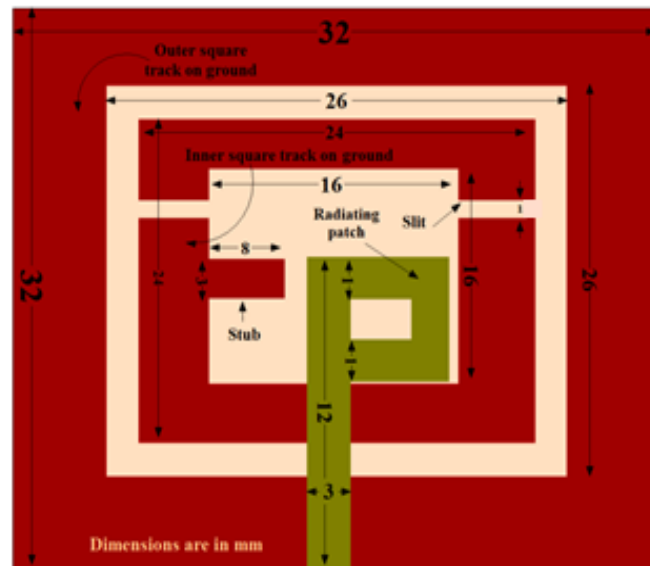


**Fig. 1** Geometrical top (green color) and bottom (red color) view of the proposed structure

To better understand the behavior of the proposed design, stepwise growth of the proposed design in five different steps are displayed in terms of reflection coefficient, gain and axial ratio (Fig. 3). The antenna design- $A_5$  is best suited on the basis of the simulated results for C and X-band applications. The geometrical structure with physical dimensions and fabricated photograph of the proposed antenna ( $A_5$ ) are shown in Fig. 1 and Fig. 2(a)-(b) respectively. Various antenna parameters such as reflection coefficient, gain, axial ratio, current distribution and radiation pattern have been analyzed in simulation environment.

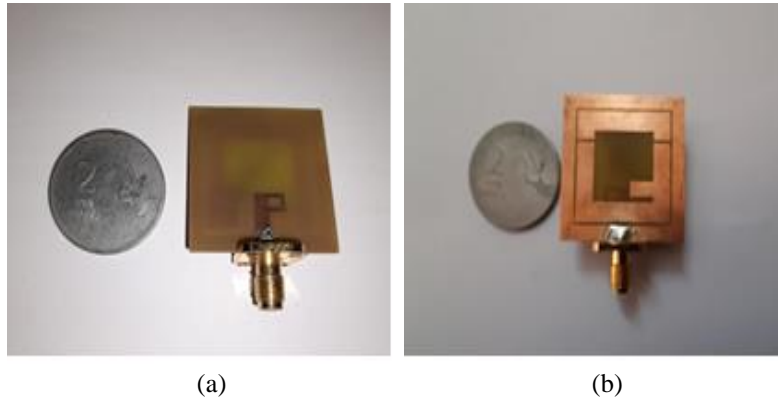


**Fig. 2** Top (a) and bottom (b) view of the fabricated antenna

## 2. EVOLUTION OF ANTENNA DESIGN

The evolution/stepwise growth (Table 1) of the proposed design is self explanatory. Defects created on the ground have been parametrically analyzed to get the optimized dimensions of the antenna and antenna parameters. Effect of square track (2 mm thick), inner square slot (16 mm×16 mm), slit (1 mm×24 mm) and perturbation (3 mm×8 mm) created on the ground from antenna A1-A5 is observed in simulation environment. It is clear from Fig. 3(a-c) that antenna A1 exhibits resonating band (10.4-10.6 GHz) with maximum gain of 4.57 dBi and without usable axial ratio band. Increment in resonating bands are observed by creating square track/defect on the ground of antenna A1 (results antenna A2). Antenna A2 does not carry sufficient gain within the bands. Change in inductive and capacitive effect of input impedance created by square track/defect is the main reason of change in return loss, axial ratio and gain. Electromagnetic coupling may also be the reason of change in antenna parameters. Further square slot (16 mm×16 mm) is etched from ground of antenna A2 to obtain antenna A3 for improving the gain within the resonating and axial ratio band. Antenna A4 is obtained by introducing the slit (1 mm×24 mm) in antenna A3 which creates the electromagnetic coupling gap in the inner ground. Finally, antenna A5 (proposed antenna) is obtained by adding the perturbation in lower left corner of antenna A4. Addition of perturbation alters the electric conduct of the ground which results in increment of resonating bands at higher frequency side. Resonating bands, axial ratio bands and gain of antennas A1-A5 are investigated (Fig. 3(a-c)) and tabulated in Table 1. It is clear from the Table 1 that antenna A5– proposed structure is resonating with five resonating bands but axial ratio bands (4.65-5.16 GHz) and (11.19-11.52 GHz) lie only in two resonating bands (3.37-5.60 GHz) and (10.82-11.46 GHz) with sufficient positive gain. Therefore, the proposed design (A5) is well suited for C- and X- band applications.

**Table 1** Stepwise growth and performance of proposed antenna

Antenna Shape (Name)	Resonating bands (GHz)	Gain (dBi)/ Frequency(GHz)	Axial ratio bands (GHz)
 (A <sub>1</sub> )	(10.4-10.6)	4.57/10.48	No usable band
 (A <sub>2</sub> )	(6.33-6.46) (9.38-9.72) (11.36-11.81) (12.77-13.42)	-1.7/6.46 5.59/9.68 -4.58/11.60 5.69/13.41	(9.43-9.72) (12.14-12.17)
 (A <sub>3</sub> )	(6.52-7.55)	3.09/6.58	(3.34-3.48)
 (A <sub>4</sub> )	(3.51-5.29) (6.8-7.78)	3.73/5.18 2.50/6.86	No usable band
 (A <sub>5</sub> -Proposed Antenna)	(3.37-5.60) (6.89-7.69) (9.62-9.81) (10.82-11.46) (13.36-13.58)	3.97/5.38 0.25/6.89 -0.62/9.62 0.96/11.16 1.46/13.58	(4.65-5.16) (11.19-11.52)

### 3. RESULTS AND DISCUSSION

The proposed design is imprinted on FR4 substrate (Fig. 2) and measurement is done for verification of simulation results. Anritsu Vector Network Analyzer MS2038C is used to measure the reflection coefficient ( $|S_{11}|$ ) and measurement setup used for measurement of gain, axial ratio and radiation pattern of the proposed design is shown in Fig. 6. Simulated and measured reflection coefficient and axial ratio of the proposed design is shown in Fig. 4(a).

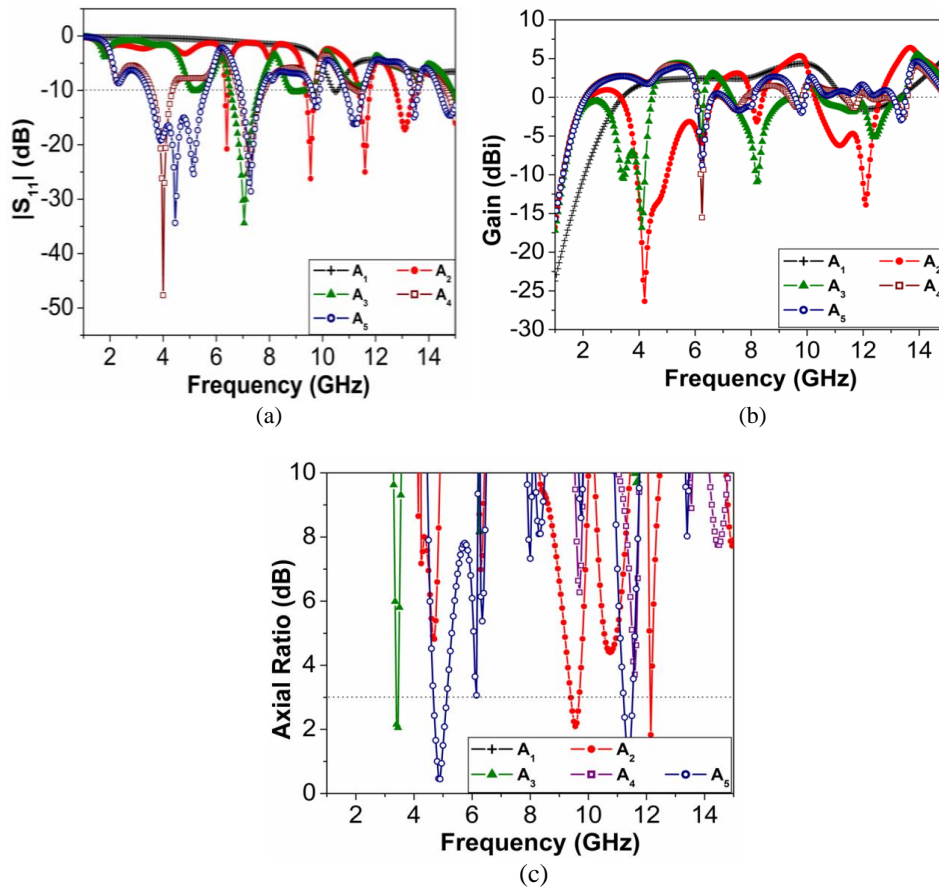


**Fig. 3** Top Parametric analysis of antenna (A<sub>1</sub>-A<sub>5</sub>) in terms of simulated (a) Return loss; (b) Gain; (c) Axial ratio

Maximum measured return loss for resonating bands (3.37-5.60 GHz) and (10.82-11.46 GHz) is -35 dB and -18 dB respectively (Fig. 4(a, b)). Measured peak gain for each resonating band is 3.97 dBi and 0.96 dBi respectively (Fig. 4(b, c)). Simulated (measured) impedance axial ratio bandwidth (Fig. 4(a,b)) of the proposed design with in axial ratio band is 10.4% (9.7%) and 2.9% (2.7%).

Simulated and measured radiation pattern for principle planes (x-z and y-z planes) at frequencies 4.85 GHz and 11.4 GHz are displayed in Fig. 5. Bidirectional radiation pattern with right hand circular polarization (RHCP) in +Z direction and left hand circular polarization (LHCP) in -Z direction is observed from Fig. 7. Radiation patterns are little bit distorted from principle axis which may be due to asymmetry in the proposed structure with respect to y-axis. It is clear from Fig. 5 that the difference (for both simulated and measured) between RHCP and LHCP component is more than 10 dB for both frequencies and planes.

Simulated surface current distributions at frequencies 4.96 GHz and 11.4 GHz shown in Fig. 7 validate the circular polarization of the proposed design. Surface current distributions are simulated using HFSS version 13 from  $0^\circ$  to  $270^\circ$  with advancement of  $90^\circ$ . It is observed from Fig. 7 that the direction of surface current reverses when phase changes from  $0^\circ$  to  $180^\circ$  and  $90^\circ$  to  $270^\circ$  respectively. It can also be seen from Fig. 7 that X and Y magnitude are almost equal with phase difference of  $90^\circ$  in radiating patch which satisfies the necessary condition for generation of circularly polarized waves. It is confirmed from Fig. 7 that current is rotating in anticlockwise direction and clockwise direction with respect to +Z direction at frequencies 4.96 GHz and 11.4 GHz respectively which confirms the RHCP and LHCP waves at frequencies 4.96 GHz and 11.4 GHz respectively.

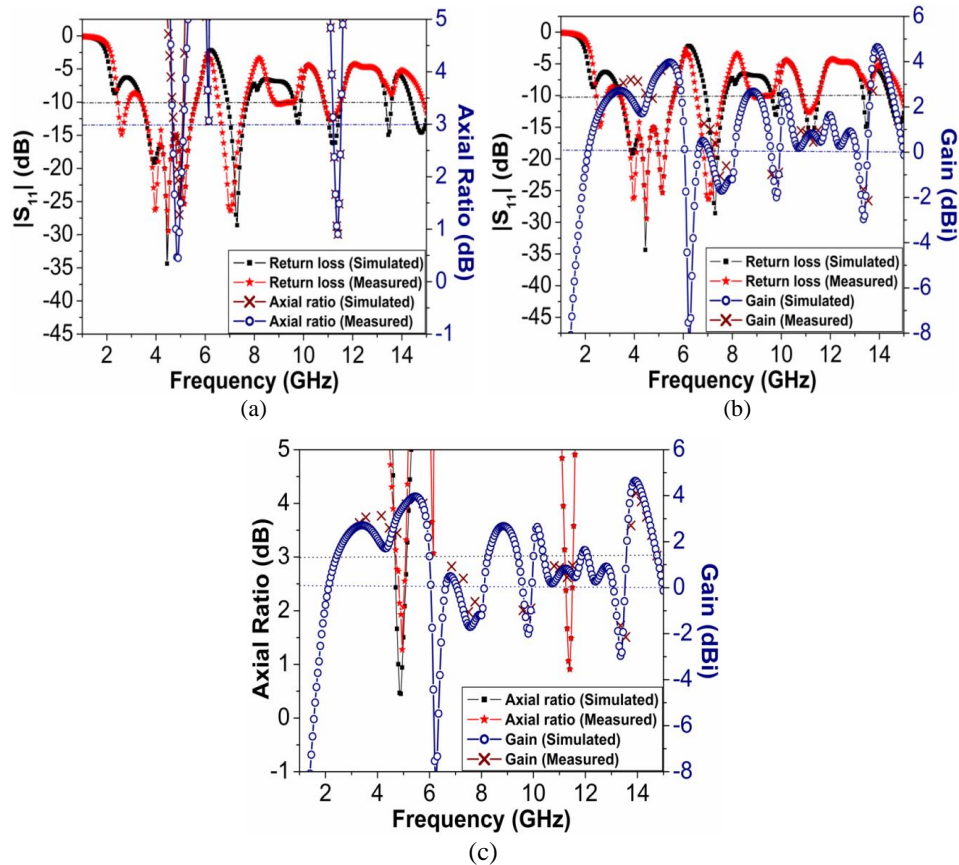


**Fig. 4** Simulated and measured result of proposed antenna in terms of (a) Return loss and axial ratio; (b) Return loss and gain; (c) Axial ratio and gain

A comparison of previously reported circularly polarized dual band antennas is established in Table 2 in terms of material/substrate, resonating bands, impedance bandwidth, AR bands, Impedance ARBW, peak gain and applications. It can be observed from Table 2 that dielectric resonator [16-18] and FR4 substrate [19-20] are used for getting dual band circularly polarized

antenna for different applications. The reported literatures in Table 2 cover either WLAN/WiMAX or C-and X-band applications. It is clearly depicted in Table 2 that the proposed antenna along with [18-20] offers two circularly polarized band for C- & X-band applications. Proposed antenna also offers smallest area ( $32 \times 32 \text{ mm}^2$ ) except [19] ( $20 \times 20 \text{ mm}^2$ ). It is observed that antenna which covers full downlink frequency (3.74-4.2 GHz) and X-band has not been encountered in Table 2 except [18]. So the proposed design is novel in the sense that it covers C- and X -band with sufficient gain, impedance bandwidth and smallest area which is useful for aeronautical mobile, fixed land mobile broad casting and fixed mobile and satellite communication.

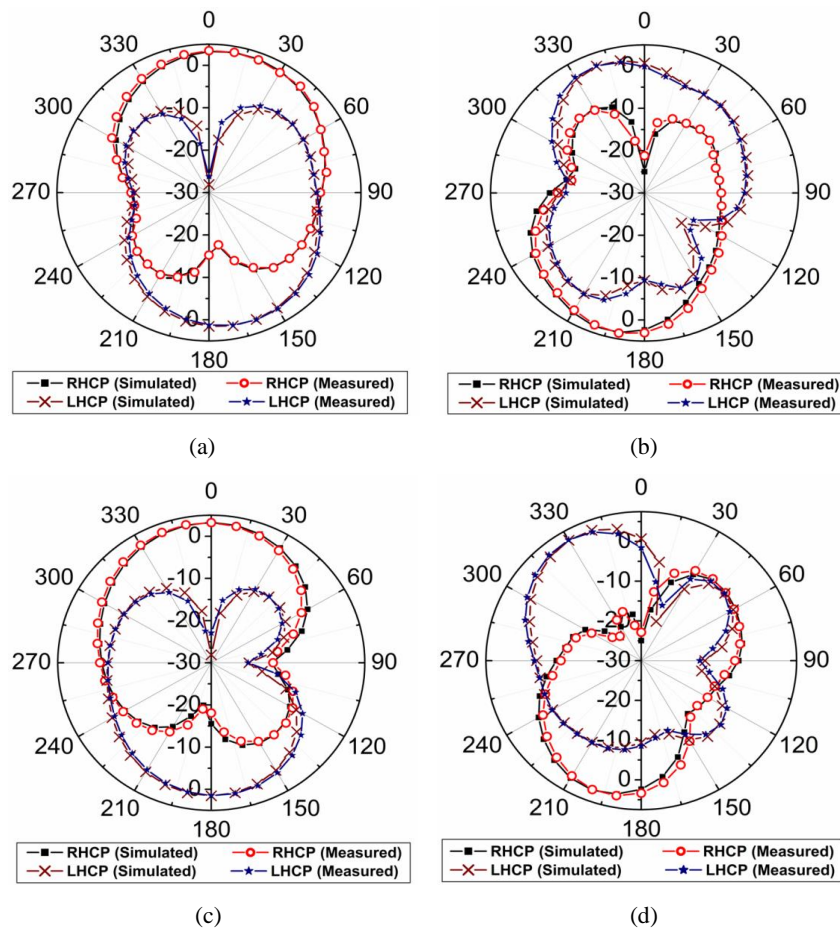


**Fig. 5** Radiation pattern of the proposed CP antenna in the x-z plane at (a) 4.96 GHz; (b) 11.4 GHz and in the y-z plane at (c) 4.96 GHz (d) 11.4 GHz

**Table 2** Comparison of proposed antenna with other circularly polarized antennas

Ref.	Material/ Substrate	Resonating bands (GHz)	IBW (%)	AR bands (GHz)	Impedance ARBW (%)	Peak Gain (dBi)	Applicatio ns
[16]	Ring dielectric resonator	(2.88–3.72) (5.4-5.95)	25.4 9.6	(3.0–3.4) (5.64-5.98)	9.52 5.85	6	WLAN and WiMAX
[17]	Cylindrical dielectric resonator	(2.4-2.90) (4.9- 5.98)	18.04 19.85	(2.55-2.72) (4.9-5.68)	6.45 14.74	7	WLAN and WiMAX
[18]	Hybrid ring cylindrical dielectric resonator	(3.4-4.18) (7.25- 9.74)	20.58 29.31	(3.92-4.08) (8.85-9.61)	4 8.23	5.8 8.2	C and X band
[19]	FR4	(4.94-9.42)	62.39	(5.94-6.69) (7.77-8.86) (6.89-6.99)	11.75 13.12 1.37	4.8	C and X band
[20]	FR4	(4.48-10.12)	80.53	(7.84-8.03) (8.83-8.98)	2.35 1.67	5.9	C and X band
[*]	FR4	(3.37-5.60) (10.82-11.46)	50.7 5.7	(4.65-5.13) (11.21-11.52)	9.7 2.7	3.9 0.9	C and X band

[\*]-Proposed structure, AR-Axial Ratio, ARBW-Axial Ratio Band Width, IBW-Impedance Band Width



**Fig. 6** Measurement setup for gain, axial ratio and radiation pattern of the proposed antenna in anechoic chamber

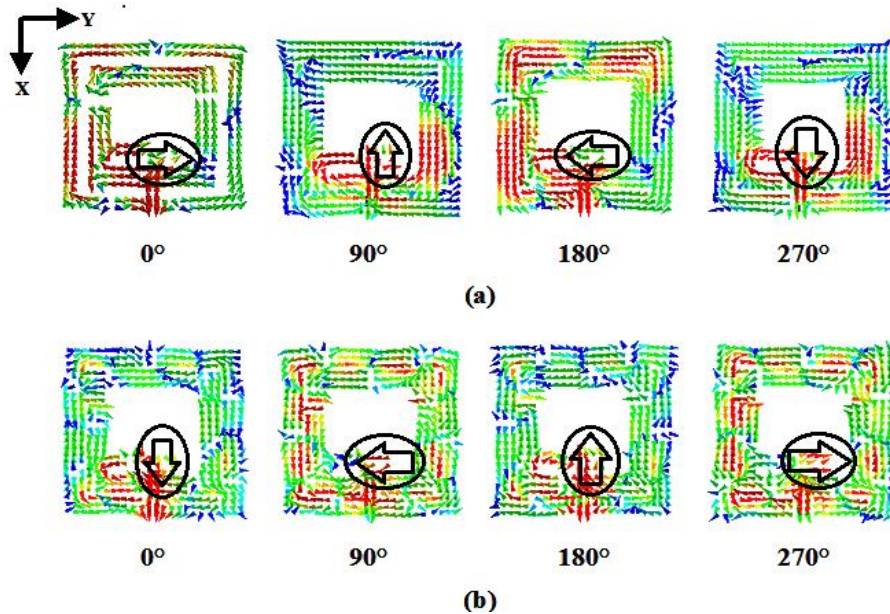


Fig. 7 Surface current distribution with  $90^\circ$  phase shifts for (a) 4.96 GHz; (b) 11.4 GHz.

#### 4. CONCLUSIONS

In this paper, the design of novel circularly polarized antenna for wireless applications is presented. Defects (square track, square slot, slit and perturbation) in ground plane is responsible for circular polarization at lower (4.65-5.13 GHz) as well as higher (11.21-11.52 GHz) frequency bands. RHCP and LHCP waves are offered within 3 dB axial ratio bands with measured axial ratio impedance bandwidth of 9.7% and 2.7% at frequencies 4.96 GHz and 11.38 GHz respectively. Compactness and mentioned characteristics of the antenna makes it suitable for aeronautical mobile, fixed land mobile broad casting, and fixed mobile except aeronautical mobile.

#### REFERENCES

- [1] A. Ghorbani, M. Ansarizadeh and R. A. Abd-Alhameed, "Bandwidth limitations on linearly polarized micro-strip antennas", *IEEE Trans. Antennas Propag.*, vol. 58, no. 2, pp. 250-257, 2010.
- [2] C. A. Balanis, *Antenna Theory Analysis and Design*, 3rd edition. New York, NY: Wiley-Inter Science, 2005.
- [3] C. C. Counselman, "Multipath-rejecting GPS antennas", *Proceedings of the IEEE*, vol. 87, no. 1, pp. 86-91, 1999.
- [4] K. Srivastava, S. Singh, A. Singh and R. Singh, "Dual band integrated wideband multi resonating patch antenna for C-band and Ku-band applications", *Int. J. Electron. Telecommun.*, vol. 65, pp. 347-352, 2019.
- [5] M. Sano and M. Higaki, "A linearly polarized patch antenna with a continuously reconfigurable polarization plane", *IEEE Trans. Antennas Propag.*, vol. 67, no. 8, pp. 5678-5683, 2019.
- [6] K. Srivastava, A. K. Pandey, S. Singh, A. Pandey and R. Singh, "Defected circular slot dual band antenna for S, C and X-band applications", *Lect. Notes Electr. Eng.*, vol. 711, pp. 803-811, 2021.
- [7] K. Srivastava, S. Singh, A. Singh and R. Singh, "Meandered quad band antenna in rectangular slot for L/S/C/X-band applications", *Adv. Intell. Syst. Comput.*, vol. 1340, pp. 487-495, 2021.

- [8] V. V. Reddy and N. V. S. N. Sharma, "Triband circularly polarized koch fractal boundary micro-strip antenna", *IEEE Antennas Wirel. Propag. Lett.*, vol. 13, pp. 1057-1060, 2014.
- [9] M. Sano and M. Higaki, "A linearly polarized patch antenna with a continuously reconfigurable polarization plane", *IEEE Trans. Antennas Propag.*, vol. 67, no. 8, pp. 5678-5683, 2019.
- [10] R. K. Maurya, B. K. Kanaujia, A. K. Gautam, S. Chatterji and A. K. Singh, "Circularly polarized hexagonal ring micro-strip patch antenna with asymmetrical feed and DGS", *Microw. Opt. Technol. Lett.*, vol. 62, no. 4, pp. 1702-1708, 2020.
- [11] X. Ding, Z. Zhao, L. Zhou, M. S. Ellis, Z-P. Nie, "Dual-band dual sense unidirectional circularly polarized antenna with CPW-fed for wireless applications", *Prog. Electromagn. Res. C*, vol. 55, pp. 167-177, 2014.
- [12] W-M. Li, B. Liu, H-W. Zhao, "The U-shaped structure in dual-band circularly polarized slot antenna design", *IEEE Antennas Wirel. Propag. Lett.*, vol. 13, pp. 447-450, 2014.
- [13] C.-J. Wang and Y.-W. Cheng, "A CPW-fed micro-strip fork-shaped antenna with dual-band circular polarization", *Prog. Electromagn. Res. C*, vol. 66, pp. 173-182, 2016.
- [14] K. Kandasamy, B. Majumder, J. Mukherjee and K. P. Ray, "Dual-band circularly polarized split ring resonators loaded square slot antenna", *IEEE Trans. Antennas Propag.*, vol. 64, no. 8, pp. 3640-3645, 2016.
- [15] K. Srivastava, B. Mishra and R. Singh, "Stub-matched inverted L-shape circularly polarized antenna for C-band applications", *Int. J. Microw. Wirel. Technol.*, vol. 14, no. 4, pp. 502-510, 2022.
- [16] D. Pathak, S. K. Sharma and V. S. Kushwah, "Dual-band circularly polarized dielectric resonator antenna for wireless applications", *Int. J. RF and Microw. Comput. Aided Eng.*, vol. 28, no. 5, pp. 212-221, 2018.
- [17] A. Sharma, G. Das and R. K. Gangwar, "Dual-band circularly polarized modified circular aperture loaded cylindrical dielectric resonator antenna for wireless applications", *Microw. Opt. Technol. Lett.*, vol. 59, no. 10, pp. 2450-2457, 2017.
- [18] C. Rai, S. Singh, A. K. Singh and R. K. Verma, "Design and analysis of dual-band circularly polarized hybrid ring cylindrical dielectric resonator antenna for wireless applications in C and X-band", *Wirel. Pers. Commun.*, vol. 126, no. 2, pp. 1383-1401, 2022.
- [19] R. Dhara and T. Kundu, "Compact dual-band circularly polarized inverted y-shaped printed monopole antenna with edge ground", *Radioelectron. Commun. Syst.*, vol. 64, no. 3, pp. 125-139, 2021.
- [20] R. Dhara, S. K. Jana, M. Mitra, "Tri-band circularly polarized monopole antenna for wireless communication application", *Radioelectron. Commun. Syst.*, vol. 63, no. 4, pp. 248-260, 2020.